

Electronic Supplementary Material (ESI) for Journal of Materials Chemistry A.
This journal is © The Royal Society of Chemistry 2018

Electronic Supplementary Information (ESI) for
**Activity and Selectivity Regulation through varying the Size of
Cobalt Active Sites in Photocatalytic CO₂ Reduction**

Qiaoqiao Mu,^{‡ab} Wei Zhu,^{‡ab} Gangbin Yan,^{ab} Yuebin Lian,^{ab} Yuanzhou Yao,^{ab} Qin
Li,^{ab} Yuyu Tian,^c Peng Zhang,^c Zhao Deng^{*ab} and Yang Peng,^{*ab}

^a Soochow Institute for Energy and Materials Innovations, College of Energy, Soochow
University, Suzhou 215006, P. R. China.

^b Key Laboratory of Advanced Carbon Materials and Wearable Energy Technologies
of Jiangsu Province, Soochow University, Suzhou 215006, P. R. China.

^c State Key Lab of Metal Matrix Composites, School of Materials Science and
Engineering, Shanghai Jiao Tong University, Shanghai, 200240, P. R. China

***Corresponding author:** zdeng@suda.edu.cn (Zhao Deng);
ypeng@suda.edu.cn (Yang Peng).

[‡]These author contributed equally to this work

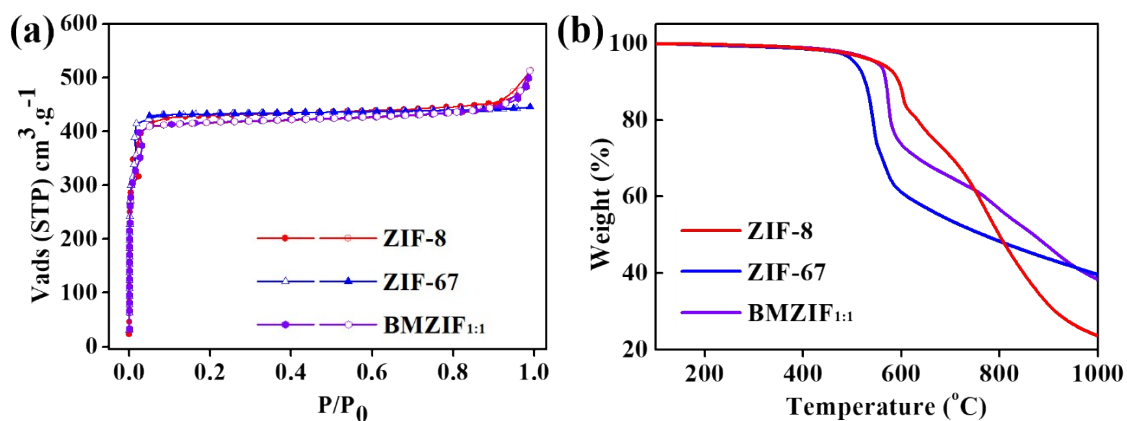


Fig. S1. (a) N₂ sorption isotherms for ZIF-8, ZIF-67 and BMZIF_{1:1} at 77 K. Filled and open symbols represent adsorption and desorption branches, respectively. (b) TGA curves of ZIF-8, ZIF-67 and BMZIF_{1:1}.

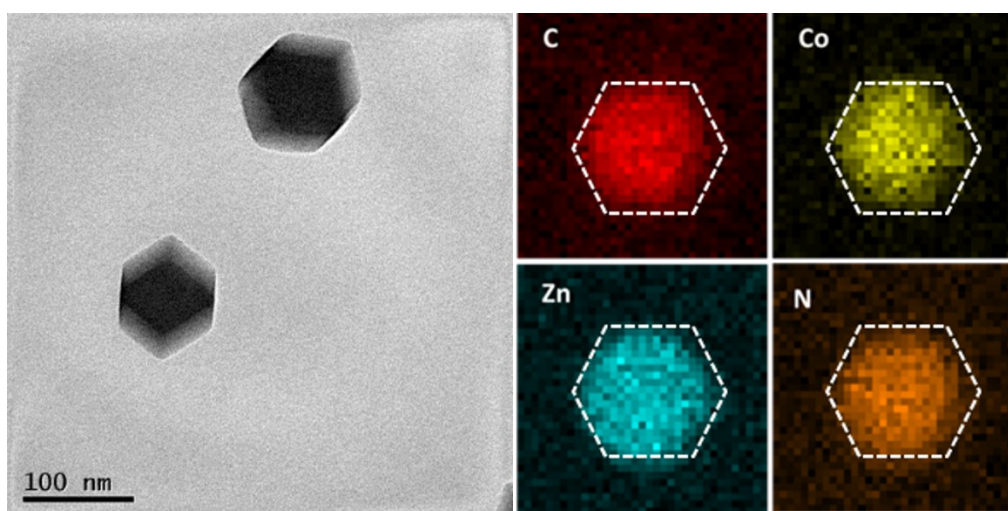


Fig. S2. TEM of BMZIF_{1:1} and the corresponding elemental mapping of C, N, Zn, Co.

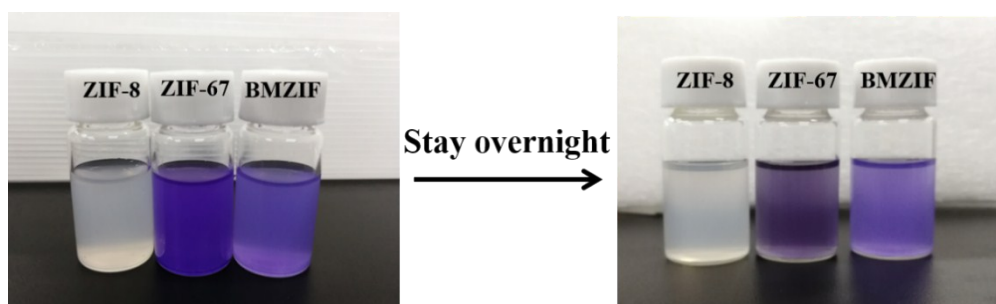


Fig. S3. The stability of ZIFs in the mixed solution of H₂O/TEOA/MeCN (2:2:10).

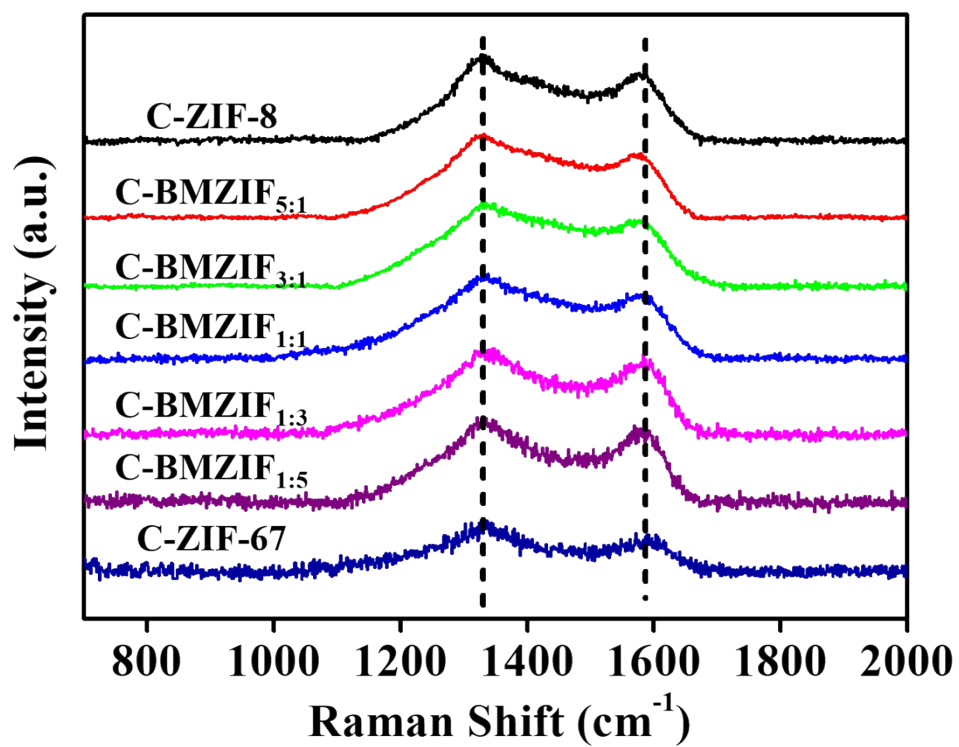


Fig. S4. Raman spectra of C-BMZIFs.

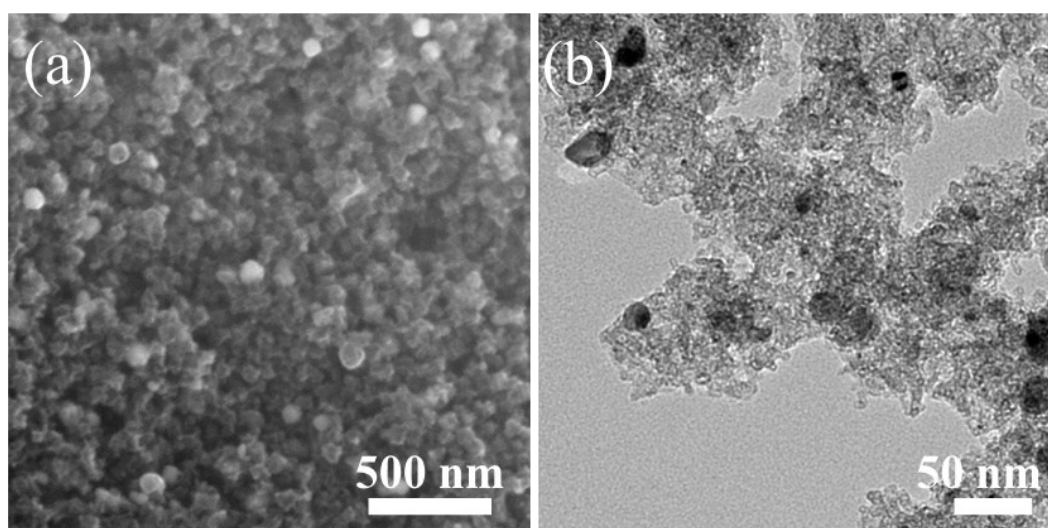


Fig. S5. SEM (a) and TEM (b) images of BMZIF_{1:1} annealed at 900°C.

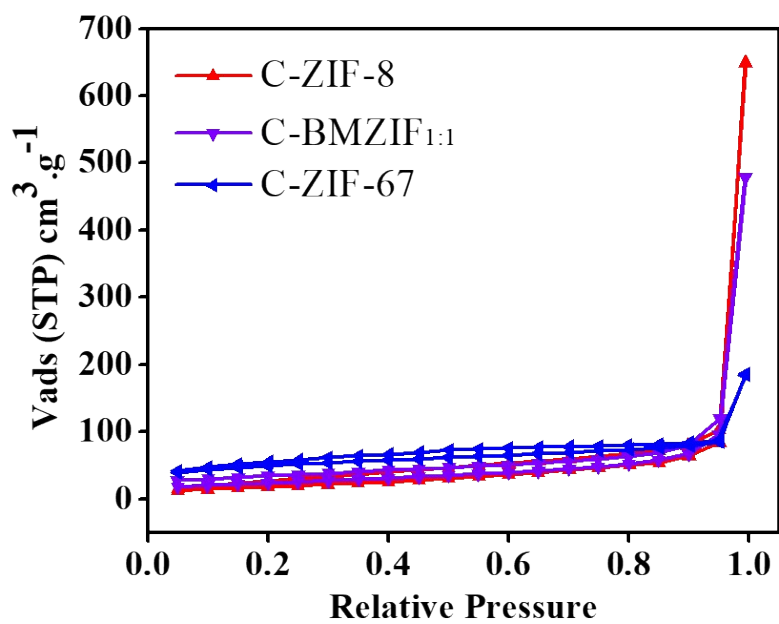


Fig. S6. N_2 sorption isotherms for C-BMZIFs at 77 K.

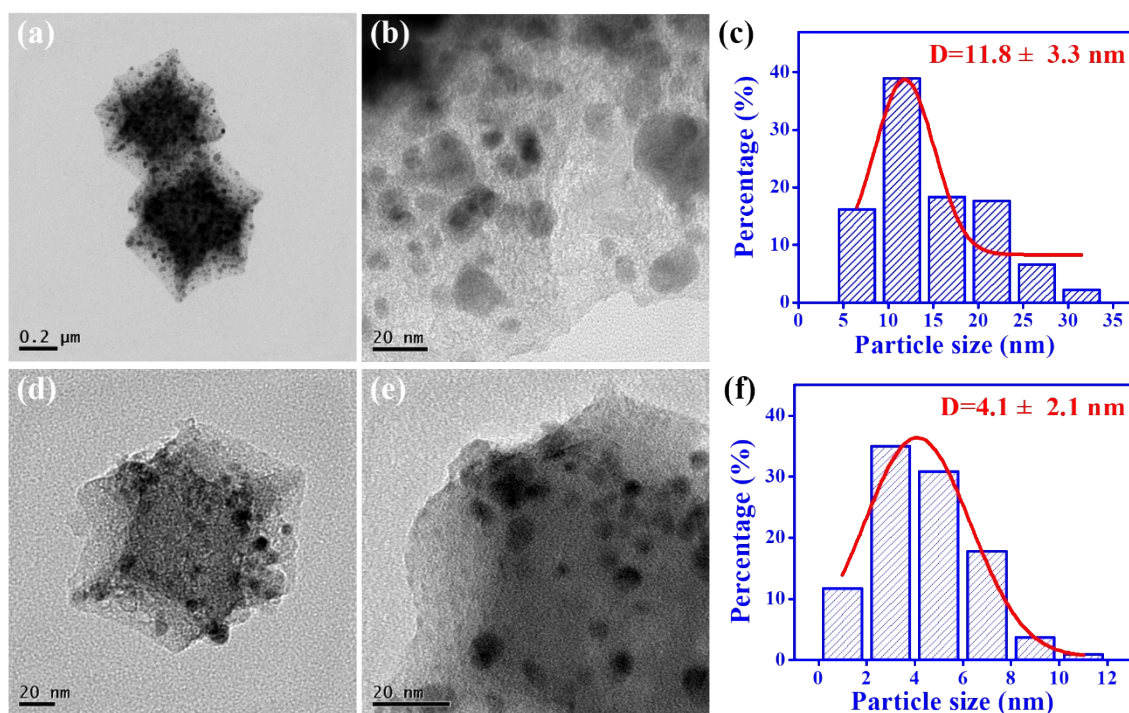


Fig. S7. TEM images of (a, b) C-ZIF-67 and (d, e) C-BMZIF_{1:1}. Cobalt particle size distributions of (c) C-ZIF-67 and (f) C-BMZIF_{1:1}.

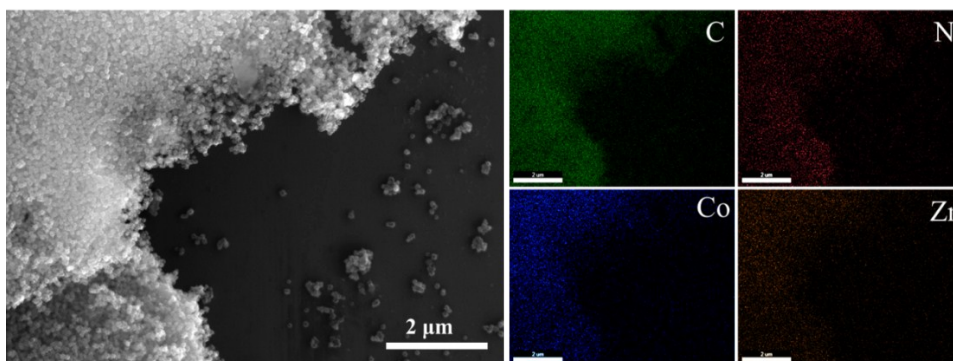


Fig. S8. Low magnification SEM of C-BMZIF_{1:1} and the corresponding elemental mapping of C, N, Zn and Co.

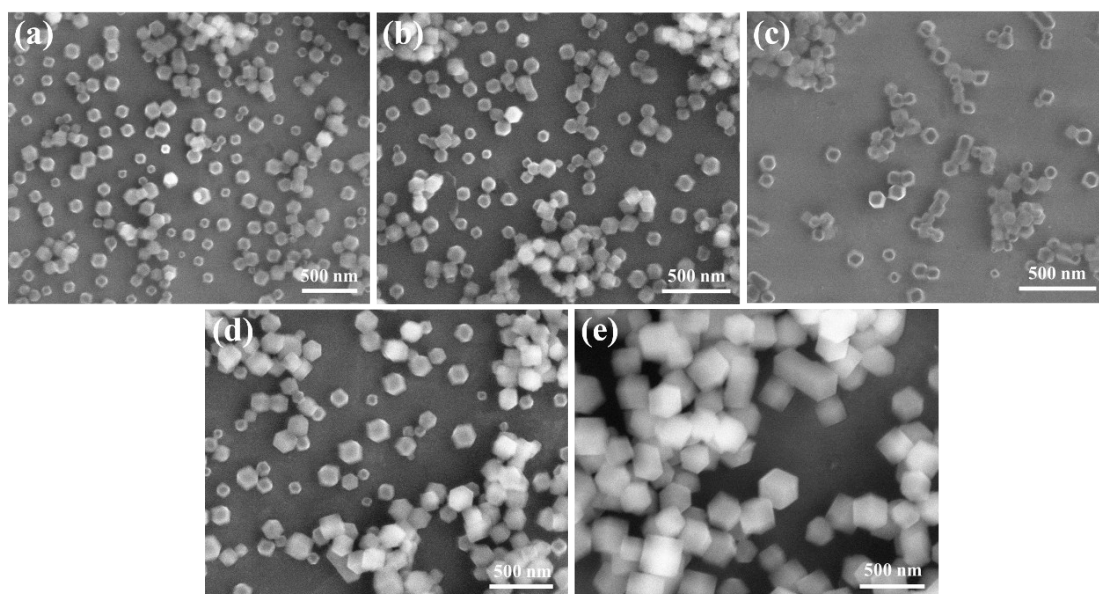


Fig. S9. SEM images of BMZIFs with different ratio of Zn/Co: (a) 5:1, (b) 3:1, (c) 1:1, (d) 1:3, (e) 1:5.

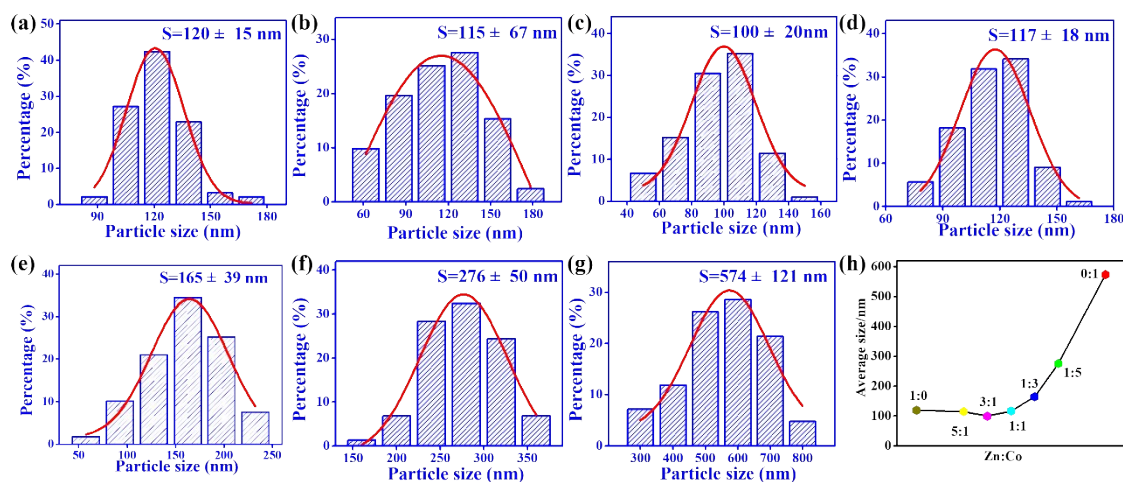


Fig. S10. Size distributions of the BMZIFs with different ratio of Zn/Co, (a) 1:0 (b) 5:1, (c) 3:1, (d) 1:1, (e) 1:3, (f) 1:5, (g) 0:1. (h) Average particle size distribution of BMZIFs.

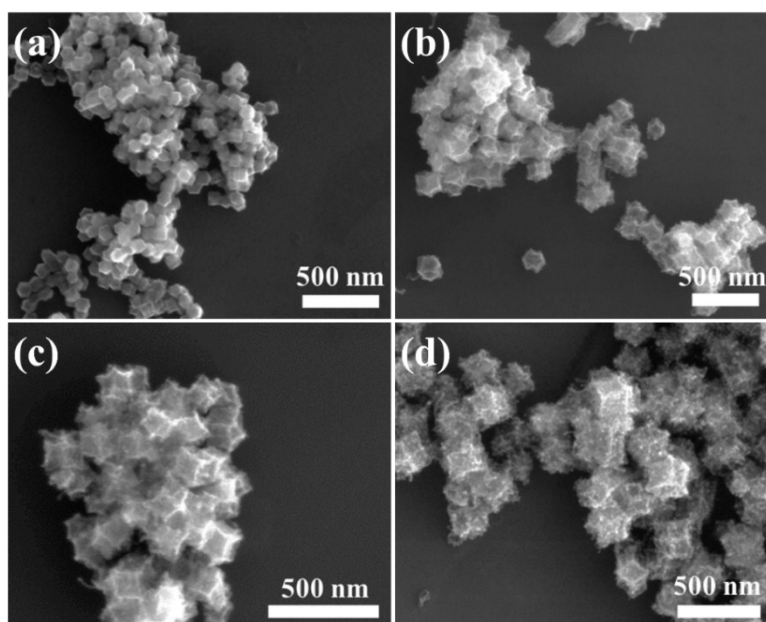


Fig. S11. SEM images of C-BMZIFs with different ratio of Zn/Co: (a) 5:1, (b) 3:1, (c) 1:3, (d) 1:5.

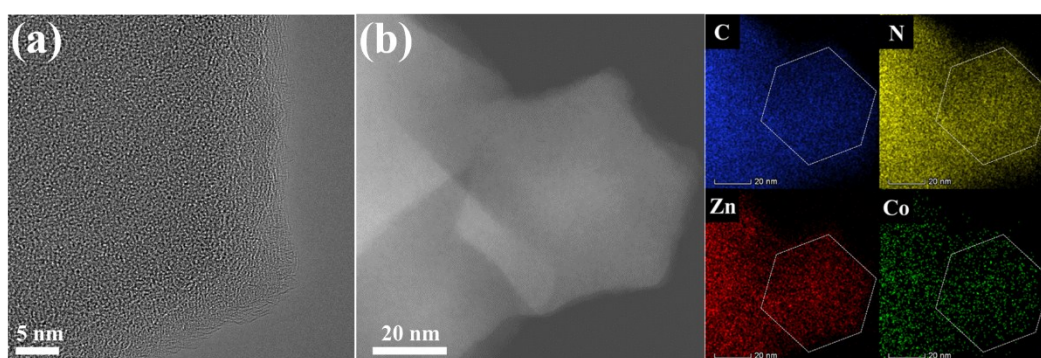


Fig. S12. (a) HRTEM image of C-BMZIF_{5:1}. (b) HAADF-STEM image and the corresponding EDS images for C, N, Zn, Co in C-BMZIF_{5:1}.

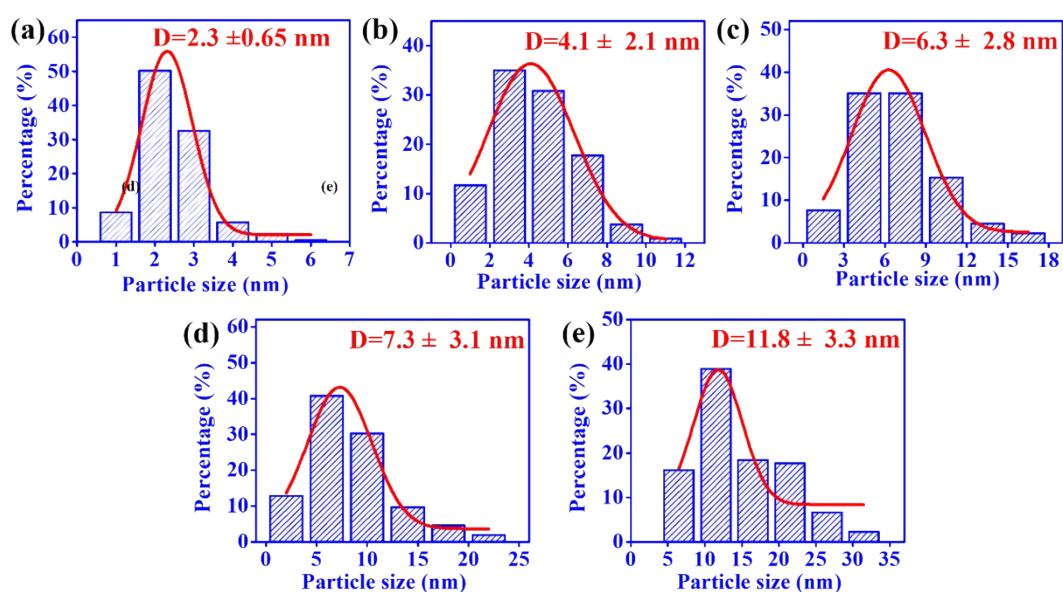


Fig. S13. Particle size distributions of Co: (a) 3:1, (b) 1:1; (c) 1:3; (d) 1:5; (e) 0:1.

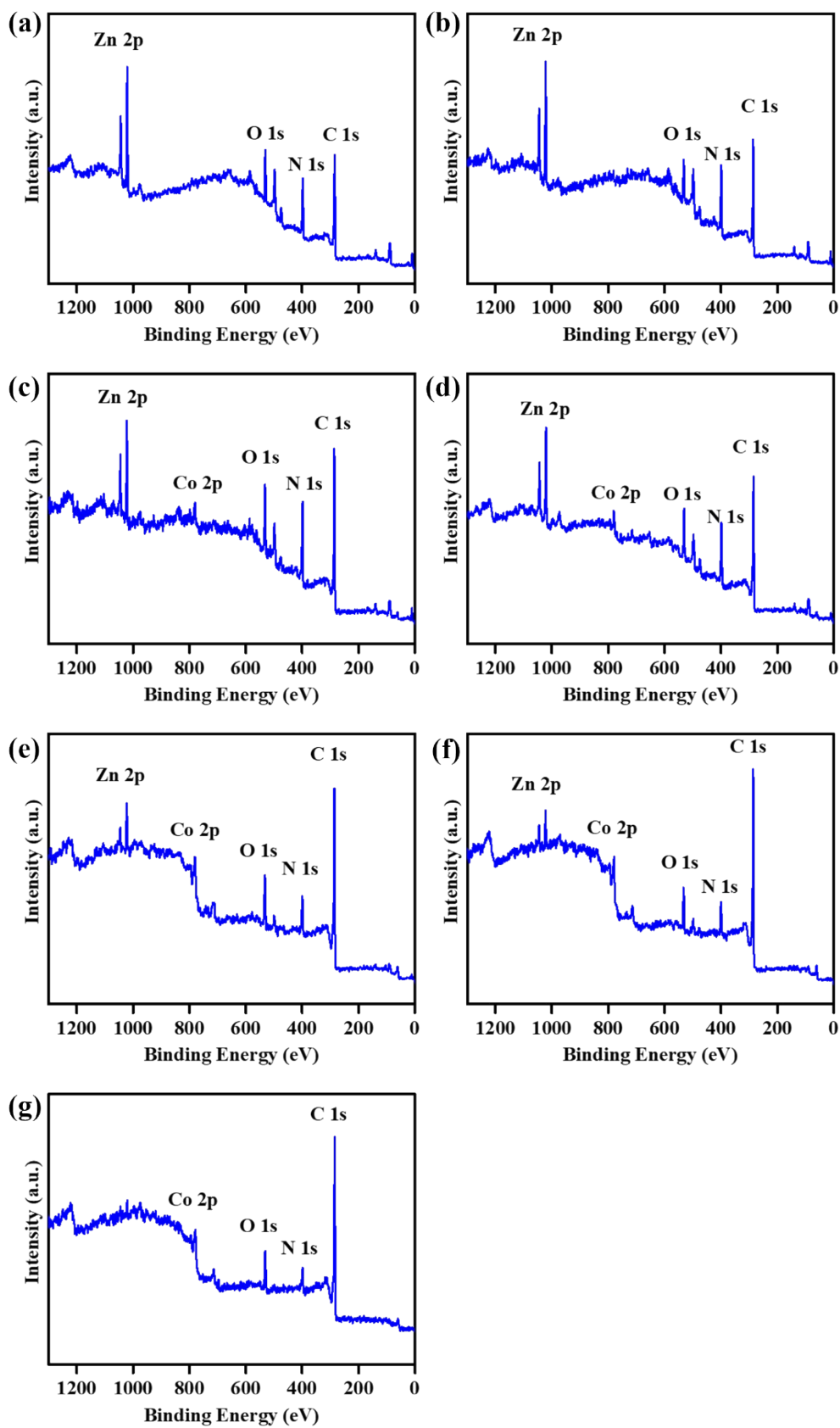


Fig. S14. XPS survey spectra of C-BMZIFs with different ratio of Zn/Co, (a) 1:0, (b) 5:1, (c) 3:1, (d) 1:1, (e) 1:3, (f) 1:5, (g) 0:1.

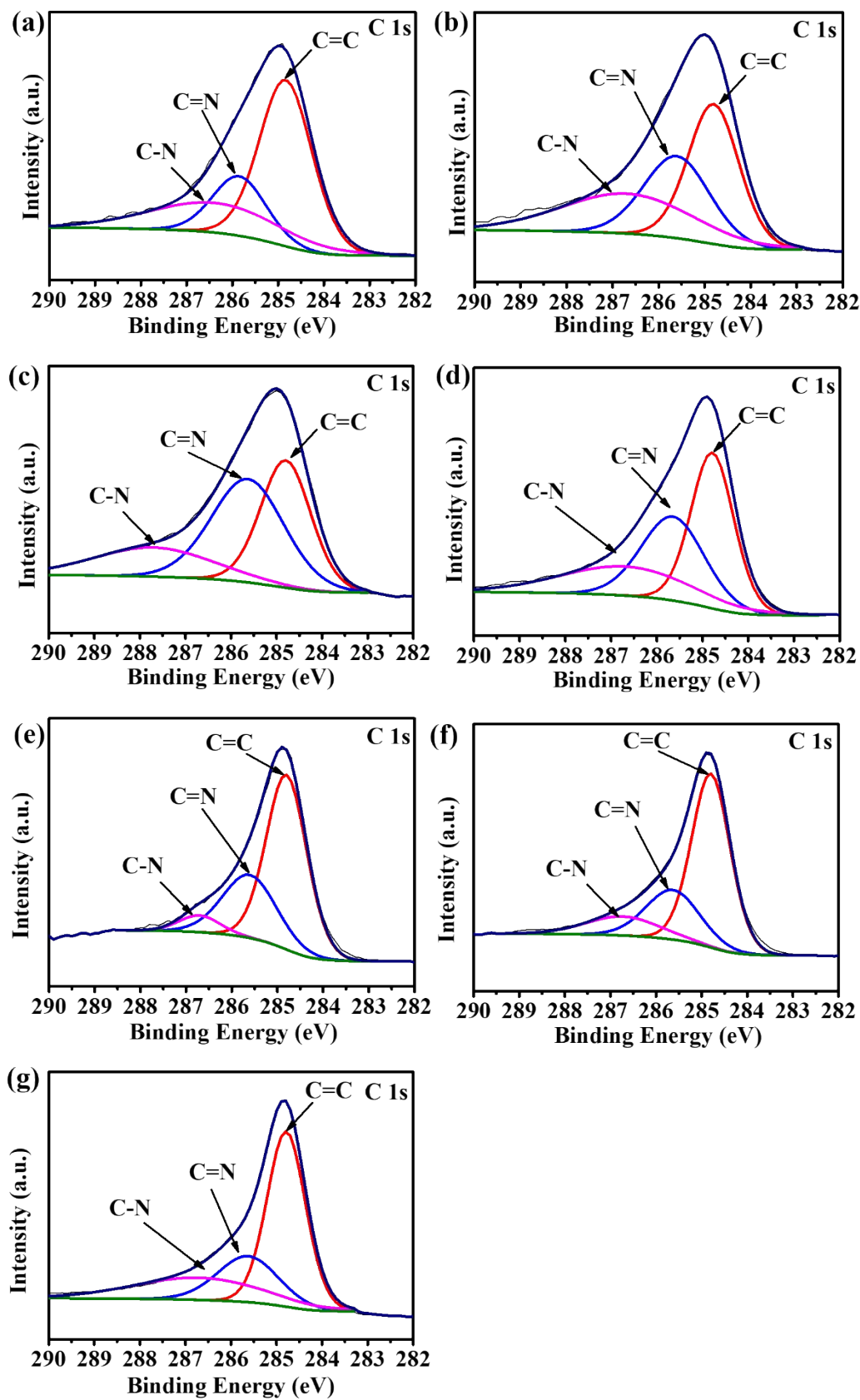


Fig. S15. High-resolution C 1s spectra of C-BMZIFs with different ratio of Zn/Co, (a) 1:0 (b) 5:1, (c) 3:1, (d) 1:1, (e) 1:3, (f) 1:5, (g) 0:1.

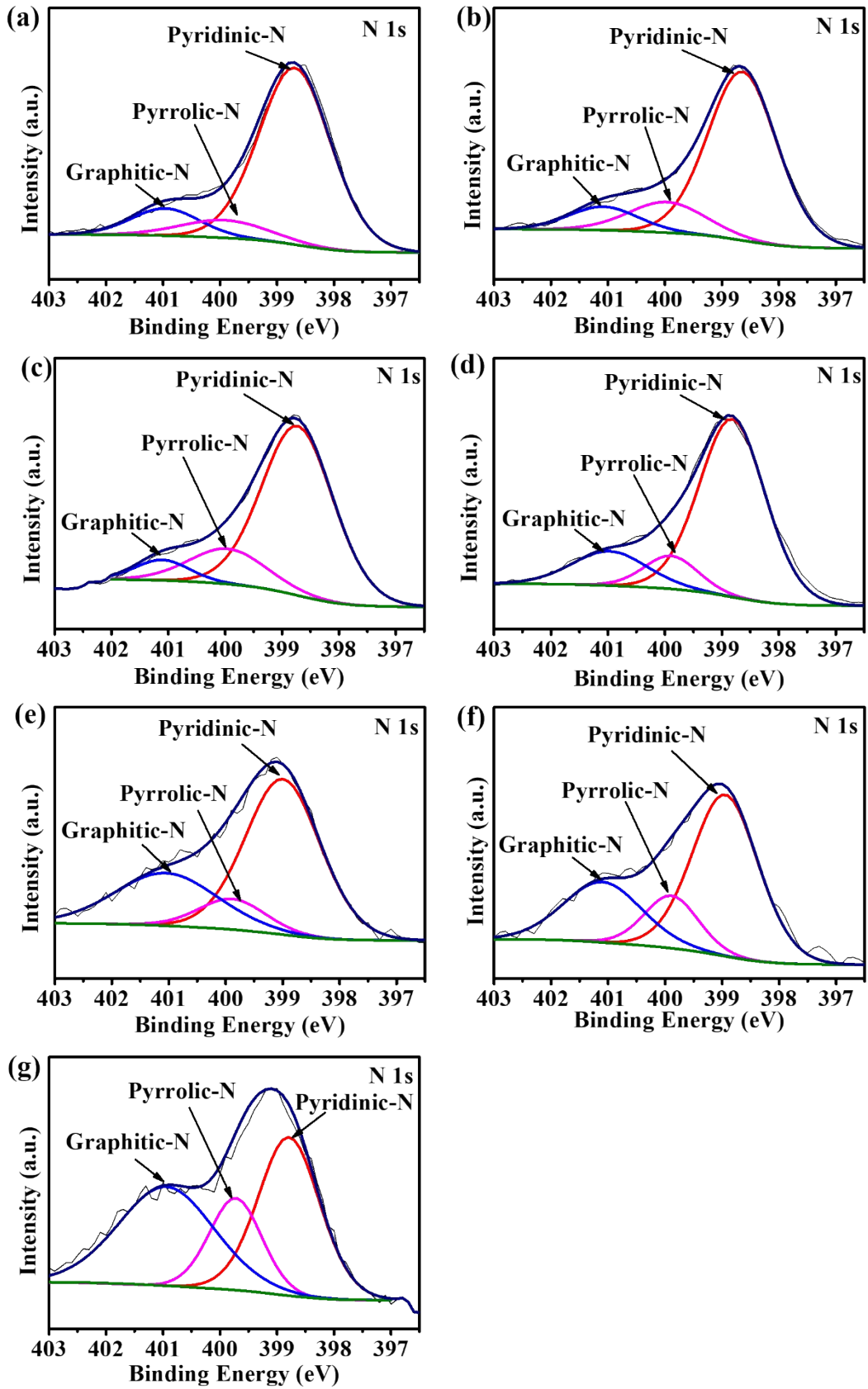


Fig. S16. High-resolution N1s spectra of C-BMZIFs with different ratio of Zn/Co, (a) 1:0 (b) 5:1, (c) 3:1, (d) 1:1, (e) 1:3, (f) 1:5, (g) 0:1.

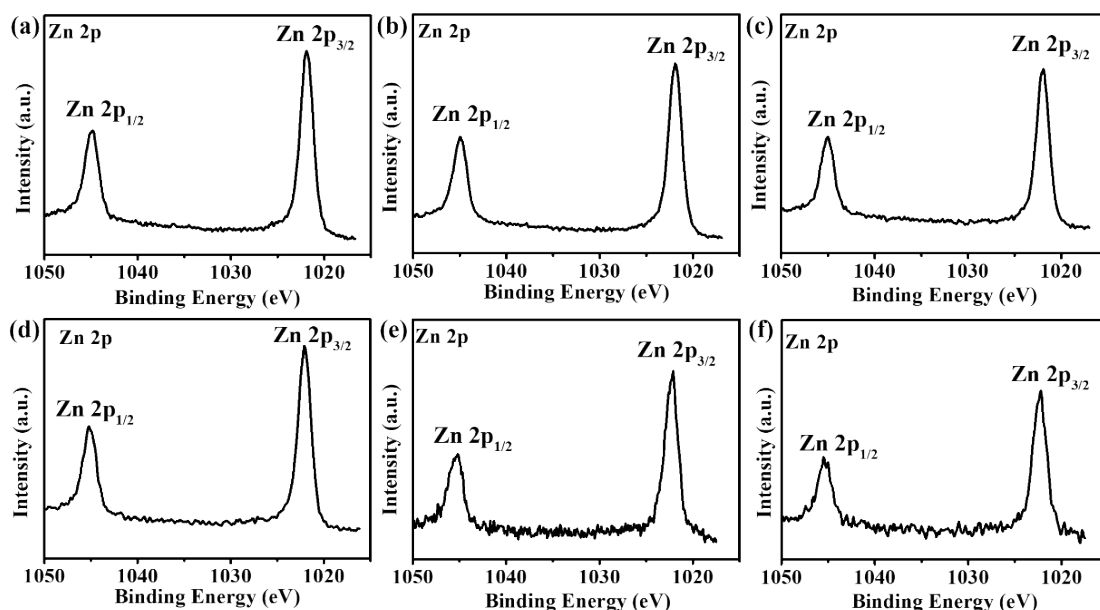


Fig. S17. High-resolution Zn 2p spectra of C-BMZIFs with different ratio of Zn/Co, (a) 1:0, (b) 5:1, (c) 3:1, (d) 1:1, (e) 1:3, (f) 1:5.

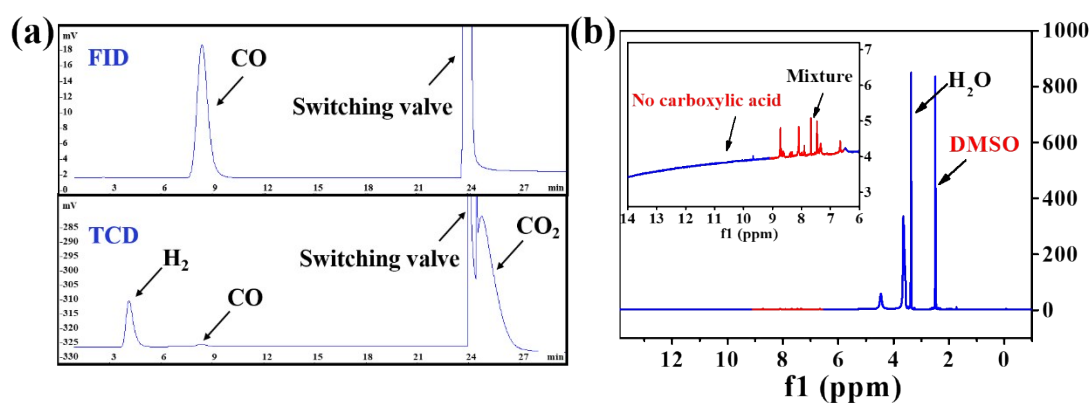


Fig. S18. (a) Products detection. GC plots of the gas products. (b) ^1H NMR of liquid products of C-BMZIF_{1:1} after photocatalytic reaction.

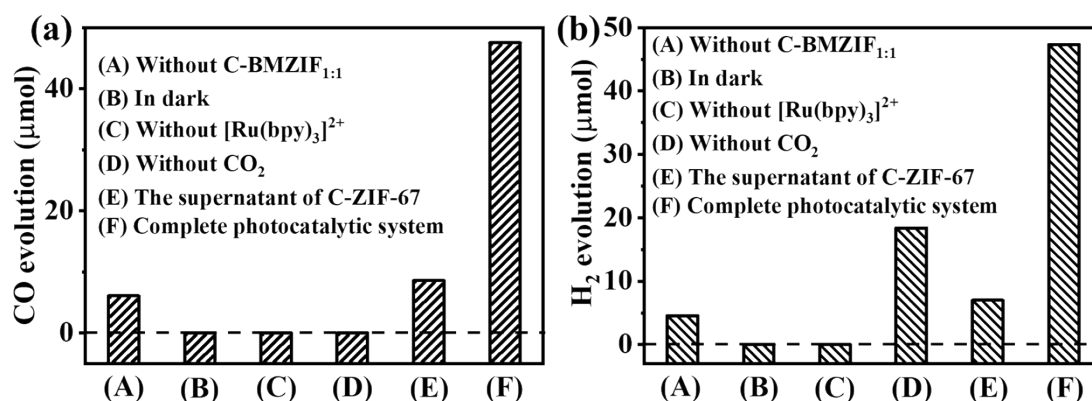


Fig. S19. (a) CO and (b) H₂ evolution vs illumination time (3 h) of the MeCN/H₂O/TEOA solution (14mL 10:2:2 v/v/v) with different control experimental conditions.

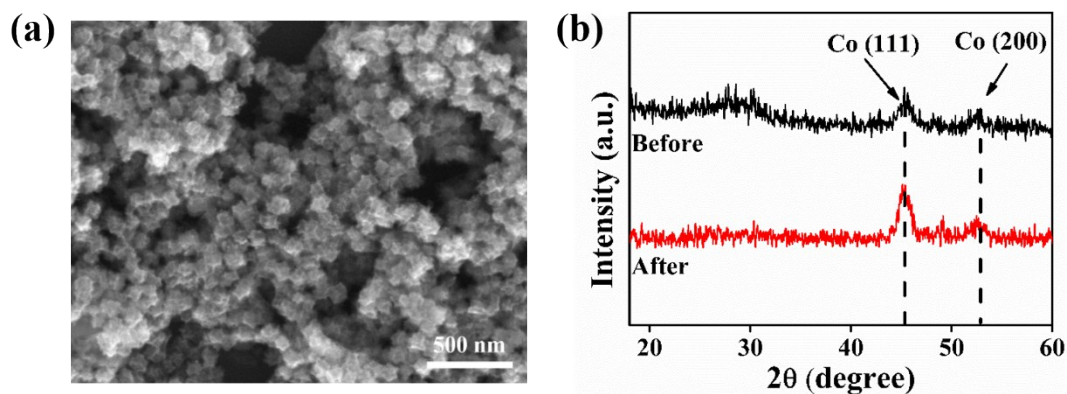


Fig. S20. The SEM image and PXRD patterns of C- BMZIF_{1:1} after photocatalytic reaction.

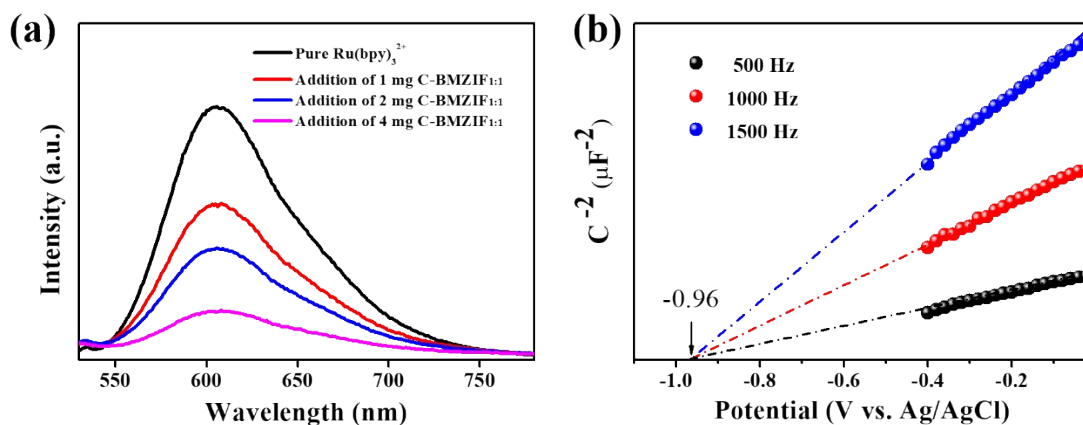


Fig. S21. (a) Photoluminescence spectra (PL) of [Ru(bpy)₃]Cl₂·6H₂O (40 mg) with different amount of C-BMZIF_{1:1} powder excited by 370 nm light. (b) Mott-Schottky plots of the C-BMZIF_{1:1} sample.

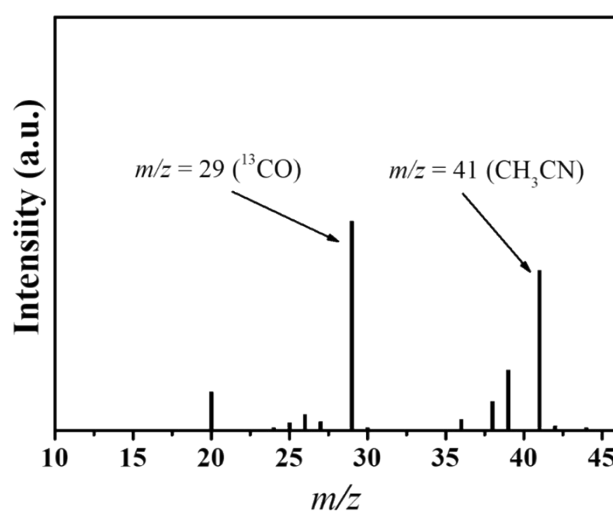


Fig. S22. Mass spectra analyses of the carbon source of the generated CO in the photochemical reduction of ¹³CO₂.

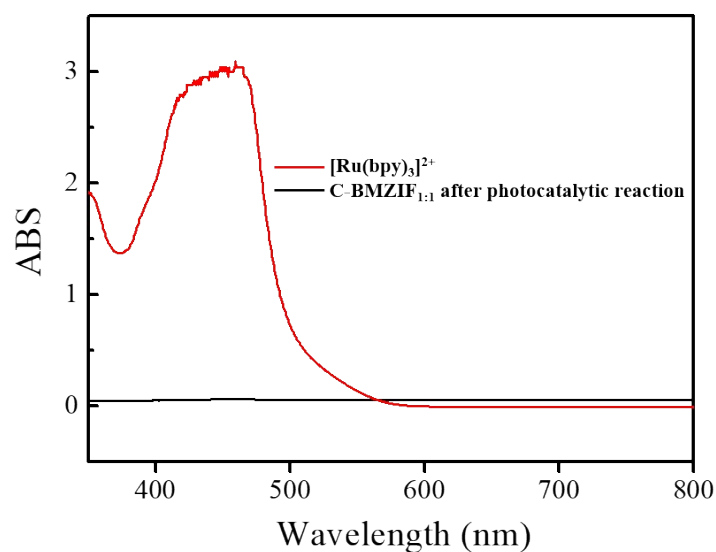


Fig. S23. The UV-vis absorption spectra of the CH_3CN solution containing $[\text{Ru}(\text{bpy})_3]^{2+}$ and C-BMZIF after photocatalytic reaction, respectively. This clearly shows the carbonized ZIFs do not absorb $[\text{Ru}(\text{bpy})_3]^{2+}$.

Table S1. The mass percentages of Co in BMZIFs and C-BMZIFs.

wt %	BMZIF _{5:1}	BMZIF _{3:1}	BMZIF _{1:1}	BMZIF _{1:3}	BMZIF _{1:5}	ZIF-67
Theoretical value						
Co	4.34%	6.52%	13.13%	19.83%	22.09%	26.64%

ICP						
Co	1.33%	3.20%	10.5%	18.05%	18.7%	27.36%

EDX						
Co	1.16%	2.39%	8.16%	14.07%	17.44%	22.93%
wt %	C-BMZIF _{5:1}	C-BMZIF _{3:1}	C-BMZIF _{1:1}	C-BMZIF _{1:3}	C-BMZIF _{1:5}	C-ZIF-67
EDX						
Co	1.74%	4.76%	10.68%	24.71%	29.18%	40.46%

Table S2. The Zn/Co molar ratio in BMZIFs and C-BMZIFs (quantified by EDX).

	BMZIF_{5:1}	BMZIF_{3:1}	BMZIF_{1:1}	BMZIF_{1:3}	BMZIF_{1:5}
Zn/Co	27.96	12.42	2.26	0.81	0.52
	C-BMZIF_{5:1}	C-BMZIF_{3:1}	C-BMZIF_{1:1}	C-BMZIF_{1:3}	C-BMZIF_{1:5}
Zn/Co	16.87	4.62	1.75	0.19	0.12

Table S3. TOF and yield of C-BMZIFs with different ratio of Zn/Co.

	C- ZIF-8	C- BMZIF_{5:1}	C- BMZIF_{3:1}	C- BMZIF_{1:1}	C- BMZIF_{1:3}	C- BMZIF_{1:5}	C- ZIF-67
Co (%) (by EDX)	-	1.74	4.76	10.68	29.18	32.87	40.46
H₂ (μmol)	3.7	21.6	41.7	47.4	50.7	52.3	56.4
Yield ($\mu\text{mol}\cdot\text{g}_{\text{cat}}^{-1}\cdot\text{h}^{-1}$)	616	3600	6950	7900	8450	8717	9400
TOF (H₂) ($\times 10^{-3}$)	-	3.4	2.4	1.2	0.47	0.43	0.38
CO (μmol)	7.2	41.3	63.8	47.5	40.2	35.9	41.7
Yield ($\mu\text{mol}\cdot\text{g}_{\text{cat}}^{-1}\cdot\text{h}^{-1}$)	1200	6883	10633	7916	6700	5983	6950
TOF (CO) ($\times 10^{-3}$)	-	6.5	3.7	1.2	0.38	0.30	0.28
Total (μmol)	10.9	62.9	105.5	94.9	90.9	88.2	98.1
TOF (total) ($\times 10^{-3}$)	-	9.9	6.1	2.4	0.85	0.73	0.66